Jagannath University Journal of Science
Volume 10, Number I, Jun. 2023, pp. 55−63
https://jnu.ac.bd/journal/portal/archives/science.jsp
ISSN 3005-4486 (Online), ISSN 2224-1698 (Print)

Possibility and Optimized Conditions for Spontaneous Superlattice Formation in Stabilized Zirconia Thin Films Grown Under *In Situ* Magnetic Field

Research Article

Nipa Debnath[1,2*], Harinarayan Das[3], Wataru Kumasaka[4], Takahiko Kawaguchi[4], Naonori Sakamoto[4,5], Kazuo Shinozaki[6], Hisao Suzuki[1,4,5] and Naoki Wakiya[1,4,5]

[1]*Graduate School of Science and Technology, Shizuoka University, Hamamatsu, 432-8561, Japan*
[2]*Department of Physics, Jagannath University, Dhaka-1100, Bangladesh*
[3]*Materials Science Division, Atomic Energy Centre, Dhaka-1000, Bangladesh*
[4]*Department of Electronics and Materials Science, Shizuoka University, Hamamatsu, 432-8561, Japan*
[5]*Research Institute of Electronics, Shizuoka University, Hamamatsu, 432-8561, Japan*
[6]*School of Materials and Chemical Technology, Tokyo Institute of Technology, Tokyo, 152-8550, Japan*

DOI: https://doi.org/10.3329/jnujsci.v10i1.71253

Received: 27 July 2023, Accepted: 12 December 2023

ABSTRACT

A specially designed, named Dynamic Aurora pulsed laser deposition (PLD) has been developed to *in situ* grow thin films in a magnetic field up to 2000 G. Spontaneous superlattice formation occurs in the case of perovskite structure ceramics due to the application of magnetic field during thin films deposition. In this study, we examine the possibility and optimize the conditions of spontaneous superlattice formation in the case of fluorite structure, stabilized zirconia thin films under *in situ* magnetic field grown by Dynamic Aurora PLD. Although, a superlattice structure was not formed in this fluorite material system. To explain this discrepancy, several factors can be considered such as the number of the cation sites in the crystal structure. Perovskite structure has two cation sites, while the fluorite structure has onlyone cation site. This study provides necessary information for further research in developing self-organized superlattice structure synthesis techniques under magnetic-field associatedpulsed laser deposition technique and simultaneously, also can play important roles in the processing of another materials system.

Keywords: *Superlattice formation, cation-sites, Dynamic aurora PLD, calcium-stabilized zirconia*

1. Introduction

In this new millennium, global warming is the most important topic of the world, that arises because of the presence of too much carbon dioxide in the atmosphere. This carbon overload is caused mainly when we burn fossil fuels like coal, oil and gas or cut down and burn forests. The solid-oxide fuel cells (SOFCs) are one of the most effective and efficient solutions to this problem and have emerged as a promising nonpolluting technology for the

***Corresponding Author:** Nipa Debnath
E-mail: nipadebnath.ju32@gmail.com

substitution of fossil fuels, which is widely used because of their high efficiency and unique scalability in electricity-generation applications (Barriocanal et al. 2008, Aoki et al. 1996). The main factor that determines the performance of SOFC is the value of the ionic conductivity of the electrolyte material. Currently, the most common electrolyte material used in SOFC has stabilized zirconia because of its mechanical stability, chemical compatibility with electrodes and high oxygen ionic conductivity. It is well established that doping ZrO_2 with oxides like Y_2O_3 or CaO stabilizes the cubic fluorite structure of ZrO_2 at room temperature and provides the oxygen vacancies responsible for ionic conduction at high temperatures. A severe drawback toward the final implementation of SOFCs is that stabilized zirconia has relatively low ionic conductivity at room temperature. Barriocanal *et al.* reported that Yttria-Stabilized Zirconia (YSZ)/ Strontium Titanite (STO) superlattice hetero-structure shows the large conductivity that basically arises from the interface of fluorite and perovskite structure (Barriocanal et al., 2008). This coherent interface in YSZ/STO superlattice structure provides both a high carrier concentration and, simultaneously, a decreased activation energy, achieving a greatly enhanced mobility that accounts for the many orders of magnitude increase of the conductivity at room temperature (Barriocanal et al. 2008). Thus, the combination of the epitaxial strain and heterogeneous interfaces appears to be a key step in the design of artificial nanostructures with high ionic conductivity. On the other hand, to improve the thermoelectric figure of merit (ZT) through the enhancement of electronic conductivity and reduction of phonon thermal conductivity, the superlattices nanostructure are now widely fabricated, investigated and applied in energy conversion devices (Ohta et al., 2007).

In general, there are two approaches to fabricating superlattice nanostructures: through artificial and self-assembly processes. However, the fabrication of superlattice structures by an artificial process is very time-consuming and costly. It has many manufacturing steps which is the barrier to practical uses on a large scale. In our laboratory we developed a specially designed pulsed laser deposition (PLD) technique, through which we can apply a magnetic field during thin film growth, named Dynamic Aurora PLD (Wakiya et al. 2007; Kubo et al. 2011; Suzuki et al. 2013; Wakiya et al. 2016, Debnath et al. 2017; Wakiya et al. 2017, Debnath et al. 2018; Lizuka et al. 2023). Spontaneous superlattice structure is formed in the case of perovskite $SrTiO_3$ (STO) system by the application of *in situ* magnetic field during film growth (Wakiya et al. 2016). From this point of view, we want to fabricate stabilized zirconia superlattice structure using Dynamic Aurora PLD through current study. We have experienced some necessary conditions for superlattice formation under *in-situ* magnetic field through the study of self-assembled perovskite structures like STO, $La_{1-x}Sr_xMnO_3$(LSMO), and $La_{1-x}Sr_xCoO_3$(LSCO) superlattice formation by Dynamic Aurora PLD (Wakiya et al. 2016; Wakiya et al. 2017; Lizuka et al., 2023). Based on these analyses, the main objective of this work is to clarify the conditions for superlattice formation in the case of fluorite structures such as stabilized zirconia.

Through this work, we realize that the superlattice formation has not been achieved in stabilized zirconia by using the self-assembled Dynamic Aurora PLD method. Though the necessary conditions which are found in the case of perovskite structure, are satisfied in fluorite structure, no superlattice formation occurs. In present study, we will also explain this discrepancy.

2. Experimental procedure

Theoretical simulation for stabilized zirconia

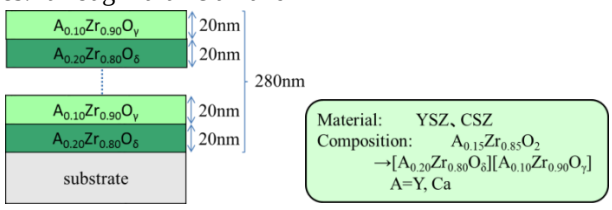

Fig. 1. A virtual model for superlattice formation in stabilized zirconia

A virtual model is proposed and presented in Figure 1. It is known that yttria-stabilized zirconia (YSZ) is the most widely used electrolytic material in SOFCs. Since, the total number of electrons in Y^{3+} and Zr^{4+} is equal, the values of the atomic scattering factor become almost equal. For this reason, if the satellite peaks are observed in the XRD pattern, it is not possible to distinguish between Y^{3+} and Zr^{4+} in each layer of the superlattice by XRD. If satellite peaks are not observed in the simulation results, it is impossible to determine whether the superlattice structure is generated by XRD analysis even when a superlattice is really generated, so it is important to perform the XRD simulation analysis for YSZ. Simultaneously we have also performed an XRD simulation for calcium oxide-stabilized zirconia (CSZ).

In the present study, we have performed the XRD simulation using the STEP model (Segmuller et al. 1973) The composition of different elements which is used for the simulation process, is given below;

YSZ: $[(Y_{0.10}Zr_{0.09}\ O_2)_{32}(Y_{0.20}\ Zr_{0.80}O_2)_{32}]_{12}$ CSZ: $[(Ca_{0.10}Zr_{0.09}\ O_2)_{32}(Ca_{0.20}\ Zr_{0.80}O_2)_{32}]_{12}$

The out-of-lattice parameter of each layer is 5.139Å. Assuming the spontaneous superlattice formation shown in Figure 1, the simulation of XRD was carried out for YSZ and CSZ systems.

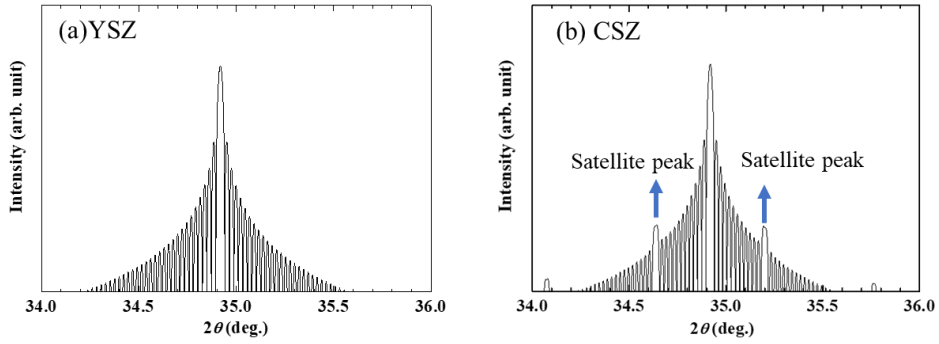

Fig. 2. Simulated XRD patterns of superlattice structure, (a) $[Y_{0.2}Zr_{0.8}]_m\ [Y_{0.1}Zr_{0.9}]_n$ (YSZ), (b)$[Ca_{0.2}Zr_{0.8}]_m\ [Ca_{0.1}Zr_{0.9}]_n$ (CSZ).

The simulated XRD patterns are presented in Figure 2 where, (a) YSZ and (b) CSZ. According to the simulation results, no satellite peaks are observed in the YSZ system while the satellite peaks should be observed in the CSZ system, as we mentioned in the previous section. The difference is ascribed to the difference of atomic scattering factors of Y^{3+} or Ca^{2+} from that of Zr^{4+}. On the basis of these results, CSZ thin films were deposited on YSZ (001) single crystal substrates by Dynamic Aurora PLD. The deposition conditions are discussed in the following section.

CSZ film deposition conditions

The experimental setup for Dynamic Aurora PLD can be found in some of our previous reports (Wakiya et al. 2007; Kubo et al. 2011; Suzuki et al. 2013, Wakiya et al. 2016, Debnath et al. 2017, Wakiya et al. 2017, Debnath et al. 2018, Lizuka et al. 2023). The direction of the induced magnetic field is parallel to the direction from the target to the substrate. Four ceramic targets of Ca-ZrO_2 were prepared with different doping amounts of Ca; where, Ca= 10, 16, 19, and 21 mol %. The target was irradiated by a KrF laser of 248 nm wavelength through a fused silica lens at a 45° elevation angle. The laser fluence was approximately 2 J/cm^2. The repetition rate was 10 Hz. The oxygen gas pressure in the vacuum was kept constant at 1×10^{-4} Torr during the entire growth period. The deposition temperature and time were, respectively, 800°C and 25 min. The crystal structure of the thin films including reciprocal space mapping (RSM) measurement was examined using a high-resolution X-ray diffractometer (HR-XRD: ATX-G; Rigaku Corp., Japan). An x-ray fluorescence spectrometer (XRFS: Minipal; PANalytical B.V., The Netherlands) was used to determine the

compositionand thickness of the films. In this study, YSZ (100) single crystal substrate and Si (100) single crystal substrate were used as the substrates. A pair of thin films were fabricated sequentially on both YSZ and Si substrates using similar deposition conditions. The films deposited on YSZ (001) were used for crystallographic measurement. The films grown on Si were utilized for measuring the composition and thickness of the films. Each substrate was immersed in 2-propanol for 30 minutes or more, degreased after oil and fat on the substrate surface, and used for film formation.

3. Results and discussion

Structural analysis

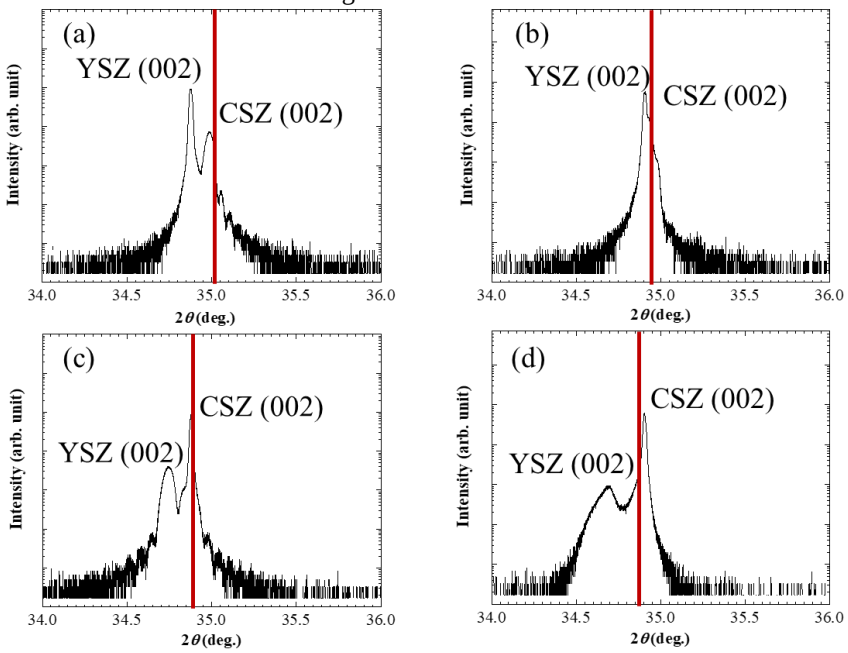

Fig. 3. XRD patterns of CSZ films (a) Ca=10 %, (b) Ca=16 %, (c) Ca=19 %, and (d) Ca=21 %,where the red line is used to indicate the peak position the CSZ thin films, is based on the theoretical lattice parameter of the CSZ thin films that is determined from the doping amount of Ca in CSZ.

In this work, the deposited four samples are named by the doping amount of Ca in CSZ such as 10 % CSZ, 16 % CSZ, 19 % CSZ, and 21 % CSZ thin films. The XRD patterns of 10 % CSZ, 16 % CSZ, 19 % CSZ, and 21 % CSZ thin films are present in Figure 3 (a), (b), (c), and (d) respectively. In all images, we used the red line to indicate the peak position of the CSZ thin films, which is based on the theoretical lattice parameter of the CSZ thin films that is determined from the doping amount of Ca in CSZ. It is well known that the lattice parameter of CSZ increases proportionally with the increase of the doping amount of Ca in CSZ (Ramírez-González et al. 2020). The lattice parameter can be calculated theoretically by the following equation Yin et al. 1993),

$$[\text{Å}] = 0.51096 + 0.015530 \times x\,(\text{CaO})$$

Where, x is the amount of Ca in CSZ. It is clearly observed from Figure 4 that the main CSZ (002) peaks in all samples are shifted to the lower 2θ angle than the peak positions fixed by theoretically calculated lattice parameters marked as red lines in images. The shift of the peak position of the CSZ thin film to the low-angle side against the theoretical peaks means that the lattice parameter of the CSZ thin film is expanded along the out-of-plane (c-axis) direction. This figure also demonstrates that no satellite peaks are detected which reveals that the superlattice formation was not formed in CSZ thin films grown under *in situ* magnetic field using Dynamic Aurora PLD.

4. Discussion (Why no superlattice is formed in CSZ thin films)

Conditions for superlattice formation

In the case of perovskite structure thin films grown by Dynamic Aurora PLD, there are three essential conditions required to be fulfilled for the spontaneous superlattice formation (Debnath et al. 2017). The three conditions are described as;

- A-site excess composition is necessary for superlattice formation.
- Coherent growth of film occurs i.e. the in-plane lattice parameter of the film and the substrate should be matched.
- The occurrence of the ion-impingement should be observed during growth time which can enhance diffusion, and reduce the activation energy for up-hill diffusion which is the characteristic of spinodal decomposition.

From Figure 2, it was confirmed that superlattice structure was not formed in A-site excess composition CSZ films grown by Dynamic Aurora PLD. According to the second condition for superlattice formation, coherent film growth should occur. Therefore, with a view to confirm whether the in-plane lattice parameter of the film and substrate is the same, reciprocal space mapping images are determined for all CSZ films (presented in Figure 4).

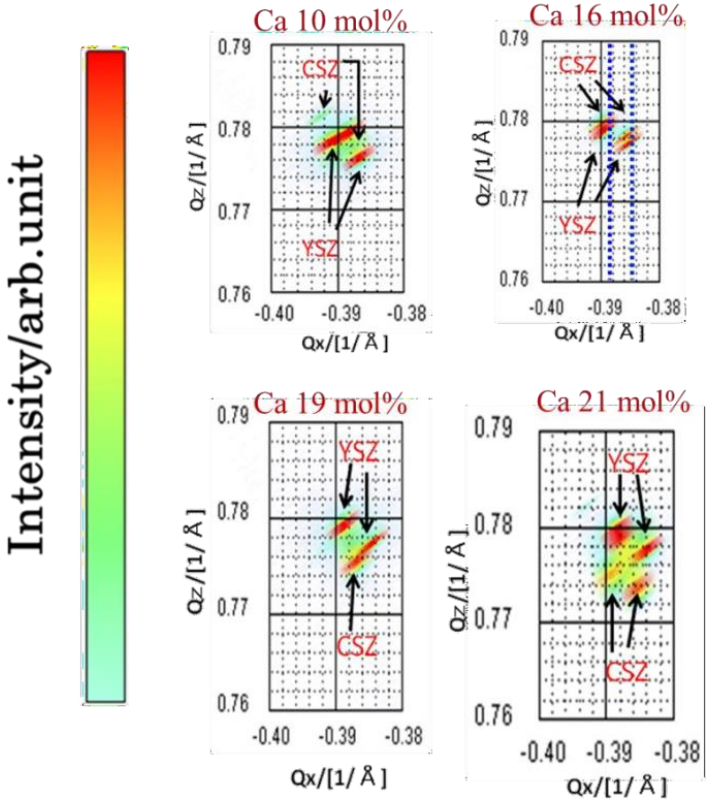

Fig. 4. Reciprocal space mapping image CSZ films where, (a) Ca=10 %, (b) Ca=16 %, (c)Ca=19 %, and (d) Ca=21 %.

Figure 4 demonstrates that only 16% Ca-doped CSZ thin film grows on the substrate coherently i.e. the in-plane lattice parameter of the film coincides with that of the substrate as shown in Figure 4 (c) indicated with blue line. But the in-plane lattice parameter of the film and substrate is not consistent for 10%, 19% and 21% Ca-doped CSZ thin films.

Analysis of the occurrence of ion-impingement under magnetic field

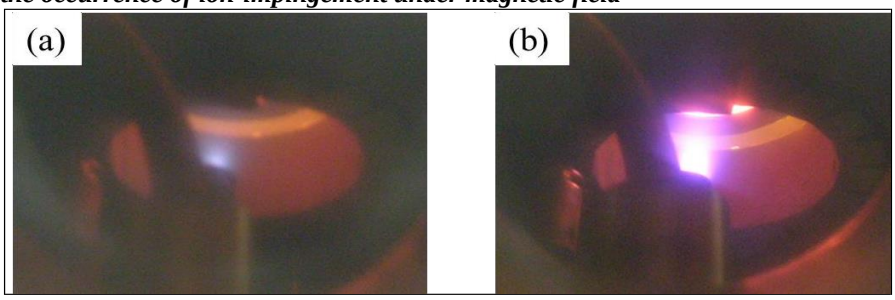

Fig. 5. General photographs of the CSZ plume under (a) 0 G and (b) 2000 G magnetic fieldwere taken during film deposition

As mentioned above, another required condition for superlattice formation by Dynamic Aurora PLD is the ion-impingement towards the substrates in the case of the perovskite structure (Wakiya et al. 2016). In this present study, it should be clarified if the ion-impingement occurs during 16% Ca-doped CSZ film deposition by Dynamic Aurora PLD. Figure 5 represents the images of plumes with and without a magnetic field. It can be observed clearly from the images that the intensity of the plume increases when a magnetic field is applied during film deposition. It has been reported that the application of a magnetic field during PLD enhances excitation and ionizationin the plume (Dirnberger et al. 1994, Lash et al. 1994, Kokai et al. 1996, Takeuchi et al. 1999, Kokai et al. 1998, Kobayashi et al. 2002, Garcia et al. 2008). Chen *et al.* have reported that ion-impingement can be induced and controlled by increasing the power of sputtering (Chen et al. 2010). In Dynamic Aurora PLD, ion impingement to the thin film during growth can be enhanced through suppression of the recombination of ions and electrons in the plume by application of a magnetic field. Here, the ablated ions and other atomic species in the plume are subjected to the Lorentz force due to the magnetic field. Because of the Lorentz force, the ions are subjected to the centripetal force, which signifies the decreaseof the divergence angle of the plume by which ionized and neutral atoms in the plume are confined toward the center of the substrate (Wakiya et al. 2016, Debnath et al. 2017). In addition, due to the magnetic field, the enhanced emission and ionization of electrons would imply an increase in the electron energy i.e. electron temperature indicating the suppression of adiabatic expansion (Dirnberger et al. 1994, Lash et al. 1994, Kokai et al. 1996, Takeuchi et al. 1999, Kokai et al. 1998, Kobayashi et al. 2002, Garcia et al. 2008). The magnetic field also suppresses the recombination of ions and electrons in the plume and ions achieve high accelerationand kinetic energy. Thus, the ions having high kinetic energy rush to the substrate and as a consequence, ion-impingement occurs (Wakiya et al. 2016, Debnath et al. 2017, Wakiya et al. 2017, Debnath et al. 2018, Lizuka et al. 2023). However, we have observed intense ion peaks in the spectra of the plume when a magnetic field was applied to the plume (Wakiya et al. 2016, Debnath et al. 2017, Wakiya et al. 2017, Debnath et al. 2018, Lizuka et al.2023).

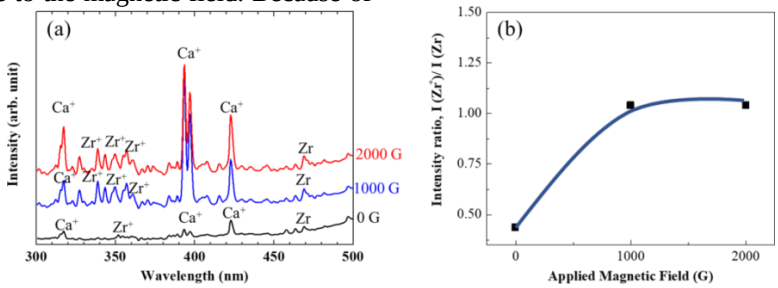

Fig. 6. (a) Emission spectra of 16% Ca doped CSZ target ablated plume at 0 G (black line), 1000 G (blue line), and 2000 G (red line) magnetic field were observed at the substrate position.

(b) The correlation between the ratio of the intensity of Zr ionized atom (Zr^+) and Zr neutral atom (Zr) and the applied magnetic field during CSZ target ablation. This graph demonstrates that the degree of ionization increases for the magnetic field application.

Figure 6 (a) presents the spectra of the ions and neutral species of the plume without and with *in situ* magnetic field when 16% Ca-doped CSZ targets are ablated. weak emission peaks from a neutral atom (Zr) and ionized atom (Ca^+, Zr^+) were observed in the plume spectra when a magnetic field have not been applied. However, strong emission peaks associated with neutral (Zr) and ionized atoms (Zr^+ and Ca^+) were observed under the application of a magnetic field during deposition. This figure indicates that the intensity of Ca^{2+} and Zr^{2+} ionized atoms increases with increasing the strength of the magnetic field. Because the spectra were measured at the substrate position ion-impingement (bombardment) occurs during thin film deposition under *in situ* magnetic field. To clarify this more quantitatively the correlation between the ratio of the intensity of the Zr ionized atom (Zr^+) and that of the Zr neutral atom (Zr) and the applied magnetic field during CSZ target ablation are expressed by plotting a graph shown in Figure 6(b). It can be demonstrated from this figure that the degree of ionization increases with applying a magnetic field. It can be said that the recombination of ions and electrons is suppressed when a magnetic field is applied to the plume. This also suggests that the application of the magnetic field during film deposition activates the plume and makes it possible to form a film in a higher energy state than the usual conventional PLD system. Therefore, ion impingement occurs during CSZ film growth by Dynamic Aurora PLD. Though the occurrence of the ion impingement is clarified and proved, superlattice structures are not formed for CSZ films grown with *in situ* magnetic fields. From the above discussion, it is noteworthy to state here that though the three conditions were satisfied in the CSZ system but the superlattice structure formation was not observed. This suggested that there may be another condition for spontaneous superlattice formation which has not been clarified yet.

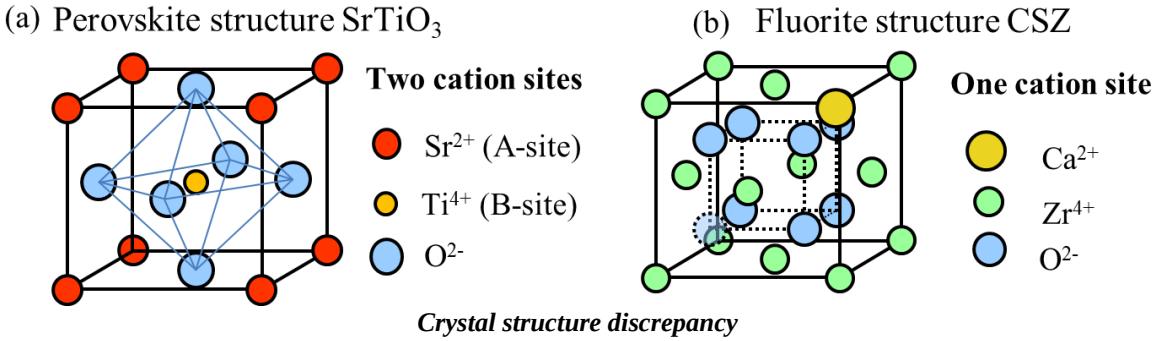

Fig. 7. Schematic crystal structure of (a) perovskite STO and (b) fluorite CSZ.

To explain the phenomenon of the spontaneous superlattice formation using the Dynamic Aurora PLD vapor epitaxy growth technique, we consider the following one possibility. The dissimilarity between the STO and CSZ material system is that STO has a perovskite crystal structure whereas, CSZ has a fluorite structure. It is known that the number of cation sites in the lattice unit cell of perovskite structure is two; A-site (Sr^{2+}) and B-site (Ti^{4+}). But, in the case of fluorite crystal structure, only one cation site (Zr^{4+}) is available in the lattice unit cell. Now, we want to clarify whether this dissimilarity of the crystal structure is related to the superlattice formation by Dynamic Aurora PLD.

In the case of STO superlattice formation under *in situ* magnetic field, A-site (Sr) excess composition is required. To explain spontaneous superlattice formation in STO, why A-site excess composition is mandatory, is discussed here first. Ohta has reported that for A-site excess STO, the formation of Ti vacancies is very unstable (Ohta et al. 2007).

Table 2 represents the energy of each species vacancy in STO, which is adopted from Reference Garcia et al. 2008. It is evident that the activation energy for Ti^{4+} vacancy is very high. The activation energy of the A-site excess composition of STO is lowered i.e. spinodal decomposition occurs to go in metastable state. When we apply a magnetic field during film growth, the ion-impingement is enhanced and reduces the activation energy, so the system easily underwent to the metastable state. Thus, it is suggested that the transition to the metastable state due to the phase separation via spinodal decomposition occurs to reduce the instability of the Ti vacancies in case of A-site excess STO. Consequently, a spontaneous superlattice structure is formed STO system by Dynamic Aurora PLD.

Table 2. Intrinsic defects in STO, data are adopted from reported reference Garcia et al. 2008,

Species	Energy [eV]
V_{Sr}^{+2}	+ 20.51
V_{Ti}^{4+}	+ 82.23
V_{o}^{2+}	+ 18.16

On the other hand, when Ca^{2+} is doped into CSZ material, the doped Ca^{2+} ion is only substituted with the Zr^{4+} cation in ZrO_2, it can be assumed that the crystal structure is relatively stable than that of STO. Therefore, transition to the metastable state does not occur, the energy barrier to the metastable state is also large which indicates the fact that maybe no spinodal decomposition occurs. For this reason, superlattice structure is not formed in CSZ thin films.

Conclusions

In conclusion, we have clarified the optimized conditions for superlattice formation in ceramic thin films under *in situ* magnetic field by Dynamic Aurora PLD. Though the stabilized zirconia thin films have been grown under optimized conditions but the superlattice structures were not found. However, the required conditions for superlattice formation in the perovskite STO system are also satisfied in the fluorite system, but superlattice formation does not occur. We observed that the perovskite crystal contains two cation sites where A-site excess compositions show superlattice formation with coherent growth with the substrate by *in situ* magnetic-field-induced ion-impingement through the spinodal decomposition mechanism which originates from the distortion or instability between two cation sites. On the other hand, there is only one cation site in fluorite structure where the Ca^{2+} cation is only replaced in the Zr^{2+} cation where the degree of up-hill diffusion is low. Therefore, in spite of satisfying the optimized conditions for superlattice formation, no superlattice structure was found in CSZ films. The results and findings of the current study helps us to investigate further in other materials system because the application of magnetic field application during thin film deposition is consequently expected to open a new avenue for progress in the field of materials science.

Acknowledgements

This work was funded by a Grant-in-Aid for Scientific Research from the Ministry of Education, Culture, Sports, Science, and Technology (No. 15H04123). Part of this work was supported by the Concert-Japan Project (FF-Photon) from the Japan Science and Technology Agency. This research is also based on the Cooperative Research Project of the Research Center for Biomedical Engineering / Research Institute of Electronics, Shizuoka University.

References

Barriocanal G, Calzada AR, Varela M, Sefrioui Z, Iborra E, Leon, Pennycook SJ, Santamaria- J. 2008. Colossal Ionic Conductivity at Interfaces of Epitaxial ZrO_2:Y_2O_3/$SrTiO_3$ Heterostructures, *Science*, 321, pp. 676-680.

Aoki M, Chiang YM, Kosacki I, Lee LJR, Tuller H, and Liu Y. 1996. Solute Segregation and Grain-Boundary Impedance in High-Purity Stabilized Zirconia, *J. Am. Ceram. Soc.*79 [5] 1169-80.

Ohta H. 2007. Thermoelectrics based on strontium titanate, *Materials Today*, 10 (10), 44-49.

Wakiya N, Muraoka K, Kadowaki T, Kiguchi T, Mizutani N, Suzuki H, and Shinozaki K. 2007. Preparation of ferromagnetic zinc-ferrite thin film by pulsed laser deposition in

the magnetic field, *J. Magn. Magn. Mater.*, 310, 2546-2548.

Kubo T, Sakamoto N, Shinozaki K, Suzuki H, and Wakiya N. 2011. Magnetic Properties of Epitaxial $NiFe_2O_4$ Thin Films Prepared Using Dynamic Aurora PLD in a Magnetic Field, *Key Eng. Mater.*, 485,221-224.

Suzuki D, Sakamoto N, Shinozaki K, Suzuki H, and Wakiya N. 2013. Magnetic field effects during deposition on crystal structure and magnetic properties of $BaFe_{12}O_{19}$ thin films prepared using PLD in the magnetic field (Dynamic aurora PLD) *Journal of the Ceramic Society of Japan* 121 [1] 45-48.

Wakiya N, Sakamoto N, Koda S, Kumasaka W, Debnath N, Kawaguchi T, Shinozaki K, and Suzuki H. 2016. Magnetic-field-induced spontaneous superlattice formation via spinodal decomposition in epitaxial strontium titanate thin films, NPG Asia Materials, 8, e279.

Debnath N, Kawaguchi T, Kumasaka W, Das H, Shinozaki K, Sakamoto N, Suzuki H, and Wakiya N. 2017. As-grown enhancement of spinodal decomposition in spinel cobalt ferrite thin films by Dynamic Aurora pulsed laser deposition, J. Magn. Magn. Mater., 432, pp. 391-395.

Wakiya N, Kawaguchi T, Sakamoto N, Das H, Shinozaki K, and Suzuki H. 2017. Progress and impact of magnetic field application during pulsed laser deposition (PLD) on ceramic thin films, Journal of the Ceramic Society of Japan, 125 [12], pp. 856-865.

Debnath N, Kawaguchi T, Das H, Suzuki S, Kumasaka W, Shinozaki K, Sakamoto N, Suzuki H, and Wakiya N. 2018. Magnetic-field-induced phase separation via spinodal decomposition in epitaxial manganese ferrite thin films, J. Science and Technology of Advanced Materials, 18, pp. 507-516.

Iizuka A, Kawaguchi T, Sakamoto N, Suzuki H, and Wakiya N. 2023. Computer simulation of spontaneous superlattice formation process by dynamic aurora pulsed laser deposition using phase field method, Journal of the Ceramic Society of Japan, 131(7), pp. 275-278.

Segmuller A and Blakeslee A. E. 1973. X-ray diffraction from one-dimensional superlattices in $GaAs_{1-x}P_x$ crystals, J. Appl. Cryst., 6, pp. 19.

Ramírez-González J, & West. A. R. 2020. Electrical properties of calcia-stabilised zirconia ceramics, Journal of the European Ceramic Society, 40(15).

Yin Y, and Argent B. B. 1993. Phase diagrams and thermodynamics of ZrO_2-CaO-MgO and MgO-CaO systems, Journal of Phase Equilibria, 14(4), pp. 439-450.

Dirnberger L, Dyer P. E, Farrar S. R and Key P. H, 1994, Appl. Phys. A 59, 311.

Lash J. S, Gilgenbach R. M, and Ching C. H. 1994. Observation of magnetic-field-enhanced excitation and ionization in the plume of KrF laser-ablated magnesium, Appl. Phys. Lett. 65, pp. 531-533.

Kokai F, Koga Y, Heimann R. B. 1996. Magnetic field enhanced growth of carbon cluster ions in the laser ablation plume of graphite, Appl. Surf. Sci. 96-98, pp. 261-266.

Takeuchi M, and Kobayashi T. 1999. Manipulation of laser plume by magnetic field application, Jpn. J. Appl. Phys. 38, pp. 3642-3645.

Kokai F, Yamamoto K, Koga Y, Fujiwara S, and Heimann R. B. 1998. Characterization of ablation plumes and carbon nitride films produced by reactive pulsed laser deposition in the presence of a magnetic field, Appl. Phys. A 66, pp. 403-406.

Kobayashi T, Akiyoshi H, and Tachiki M. 2002. Development of prominent PLD (Aurora method) suitable for high-quality and low-temperature film growth, Appl. Surf. Sci. 197-198, pp. 294-303.

García T, Posada E. de, Villagrán M, Sánchez J. L, Bartolo-Pérez P, and Peña J. L. 2008. Effects of an external magnetic field in pulsed laser deposition, Appl. Surf. Sci. 255, pp. 2200-2204.

Chen C. Q, Pei Y.T, Shaha K. P, and Hosson J. Th. M. De. 2010. Tunable self-organization of nanocomposite multilayers, Appl. Phys. Lett. 96, 073103.

Ohta H. 2007. Ceramics Japan, 42 (8), pp. 592-595.